AFRL-AFOSR-JP-TR-2016-0067

Laser Cooling of II-VI Semiconductors

Qihua Xiong
NANYANG TECHNOLOGICAL UNIVERSITY

08/12/2016
Final Report

Air Force Research Laboratory
AF Office Of Scientific Research (AFOSR)/ IOA
Arlington, Virginia 22203
Air Force Materiel Command

REPORT DOCUMENTATION PAGE

Form Approved
OMB No. 0704-0188

1. REPORT DATE *(DD-MM-YYYY)*	2. REPORT TYPE	3. DATES COVERED *(From - To)*
24-08-2016	Final	15 May 2013 to 14 May 2016

4. TITLE AND SUBTITLE
Laser Cooling of II-VI Semiconductors

5a. CONTRACT NUMBER

5b. GRANT NUMBER
FA2386-13-1-4112

5c. PROGRAM ELEMENT NUMBER
61102F

6. AUTHOR(S)
Qihua Xiong, Christian Kloc

5d. PROJECT NUMBER

5e. TASK NUMBER

5f. WORK UNIT NUMBER

7. PERFORMING ORGANIZATION NAME(S) AND ADDRESS(ES)
NANYANG TECHNOLOGICAL UNIVERSITY
50 NANYANG AVENUE
SINGAPORE, 639798 SG

8. PERFORMING ORGANIZATION REPORT NUMBER

9. SPONSORING/MONITORING AGENCY NAME(S) AND ADDRESS(ES)
AOARD
UNIT 45002
APO AP 96338-5002

10. SPONSOR/MONITOR'S ACRONYM(S)
AFRL/AFOSR IOA

11. SPONSOR/MONITOR'S REPORT NUMBER(S)
AFRL-AFOSR-JP-TR-2016-0067

12. DISTRIBUTION/AVAILABILITY STATEMENT
A DISTRIBUTION UNLIMITED: PB Public Release

13. SUPPLEMENTARY NOTES

14. ABSTRACT
The breakthrough of laser cooling in semiconductor has stimulated strong interest in further scaling up towards practical optical refrigeration. The challenge is the stoichiometric defect in bulk crystal which introduces mid-gap states that manifest as broad-band long-wavelength emission. In this project, we have developed optical floating zone method to grown millimeter-scale CdS bulk crystals. The steady-state spectroscopy measurement suggested that such defect emission prevailing in commercial CdS wafer is absent in our as-grown crystal, attributing to the low-temperature synthesis enabled by the optical heating method compared with conventional Bridgeman method. Further research is on-going to investigate the decay dynamics of the exciton emission. In addition, this project touched upon the laser cooling of inorganic-organic perovskite crystals, which are more immune to mid-gap defects.

15. SUBJECT TERMS
Laser Cooling, Optical Cooling, Bulk Semiconductors

16. SECURITY CLASSIFICATION OF:			17. LIMITATION OF ABSTRACT	18. NUMBER OF PAGES	19a. NAME OF RESPONSIBLE PERSON
a. REPORT	b. ABSTRACT	c. THIS PAGE			ROBERTSON, SCOTT
Unclassified	Unclassified	Unclassified	SAR	11	19b. TELEPHONE NUMBER *(Include area code)* +81-042-511-7008

Final Report for AOARD Grant FA2386-13-1-4112

"Laser Cooling of II-VI Semiconductors"

June 2016

Name of Principal Investigators (PI and Co-PIs):

- e-mail address : Qihua@ntu.edu.sg
- Institution : Nanyang Technological University, SPMS
- Mailing Address : 21 Nanyang Link, SPMS-04-01 Singapore 637371
- Phone : +65 513 8475
- Fax : -

Period of Performance: 05/15/2013 – 05/14/2016

Abstract: The breakthrough of laser cooling in semiconductor has stimulated strong interest in further scaling up towards practical optical refrigeration. The challenge is the stoichiometric defect in bulk crystal which introduces mid-gap states that manifest as broad-band long-wavelength emission. In this project, we have developed optical floating zone method to grown millimeter-scale CdS bulk crystals. The steady-state spectroscopy measurement suggested that such defect emission prevailing in commercial CdS wafer is absent in our as-grown crystal, attributing to the low-temperature synthesis enabled by the optical heating method compared with conventional Bridgeman method. Further research is on-going to investigate the decay dynamics of the exciton emission. In addition, this project touched upon the laser cooling of inorganic-organic perovskite crystals, which are more immune to mid-gap defects.

Introduction:

Upconversion photoluminescence (PL) is a light-matter interaction process in which the mean emission photon energy is larger than the pump photon energy. The upconversion process is facilitated by the annihilation of phonons and leads to cooling of the matter. The concept of optical refrigeration was originally proposed in 1920s, while experimentally demonstrated in rare-earth doped glasses in 1995. The latest laser cooling of rare-earth system has reached 93 K, approaching liquid nitrogen temperature. The net laser cooling in semiconductor was first demonstrated in CdS nanobelts, due to the relatively strong Froehlich interaction and more phonons available for cooling than GaAs and GaN at room temperature. As we know, in the classical Pringsheim picture for laser cooling of solid, the amount of energy in the upconversion $\Delta E = h\bar{\nu}_f - h\nu_i$ is removed in each cycle, where h is the Planck's constant, $\bar{\nu}_f$ is the mean frequency of emitted photons and ν_i is the frequency of pump photon (Fig. 1a). In addition to the large energy difference, the net laser cooling also need nearly unity external quantum efficiency (EQE) and absorption efficiency according to Sheik-Bahae/Epstein (SBE) theory.

In the achievement of net laser cooling in CdS, nanobelt morphology plays an important role in minimizing photon trapping and re-absorption, nonetheless it limits the broader applications due to sample variation and scaling challenges. Therefore, it is important to obtain bulk CdS crystals with similar optical quality towards laser cooling, which shall have important implications in macroscopic optical refrigeration devices. Unfortunately, the trapped state emission of commercial or typically synthesized CdS bulk crystals is detrimental for the laser cooling. The trapped state emission contributed by various kinds of crystalline defects would generate heat and diminish the laser cooling performance. The defect accumulation in the process of bulk crystal growth makes it more difficult to obtain ideal upconversion PL than the nanobelt due to the relative larger size.

From the above consideration, we refer to the binary compound CdS portion of Cd-S phase diagram as illustrated in Fig. 1b. Such range of homogeneity illustrated on the Fig. 1b is typical for every semiconductors, such as II-VI and III-V semiconductors. As the non-stoichiometry ranges of CdS depends on temperature, it is notable that semiconductors grown in high temperature usually has large concentration

of defects and only low temperature growth can assure stoichiometric crystals with less defects. On the other hand, however low temperature may not meet the requirement of the reaction dynamics that is needed. Chemical vapor transport used in bulk crystal growth always induces some defects due to the high temperature or impurity from the transport agent. Therefore, developing a low temperature method for crystal growth without the trapped state emission is the first challenge to achieve the laser cooling in CdS bulk crystal, which is the main goal to achieve in this AOARD project.

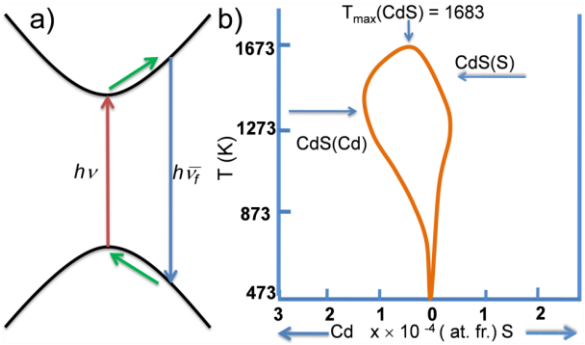

Fig. 1 (a) Laser cooling cycle by upconversion photoluminescence in a semiconductor ($h\bar{\nu}_f$ is emission photon energy; $h\nu_i$ is pump photon energy); (b) Non-stoichiometry ranges of CdS, a guideline for bulk crystal synthesis.

Experiment: Description of the experiment(s)/theory and equipment or analyses..

The Synthesis of CdS Bulk Crystal in Optical Furnace

To ensure high purity of CdS crystals we have devised a modified optical floating zone method (Crystal Systems Corporation, FZ-T-4000-H-VII-VPO-PC), which has the advantages of segregation control, crucible free and rapid growth. The source materials are sealed inside a quartz ampoule with Ar atmosphere inside. The illustration of the methods is included in the Fig. 2a. The rotation and vertical speed of displacement were set as 30 rpm and 10 mm/hr, respectively. After 30 minutes heating, the power of the lamps was decreased gradually. CdS evaporated from the hot optical focus and condensed on much colder part of CdS rod few millimeters apart from the focal point (Fig. 2b and 2c). The CdS crystal was crystallized in $P6_3mc$ space group, the same with the nanobelts used for laser cooling.

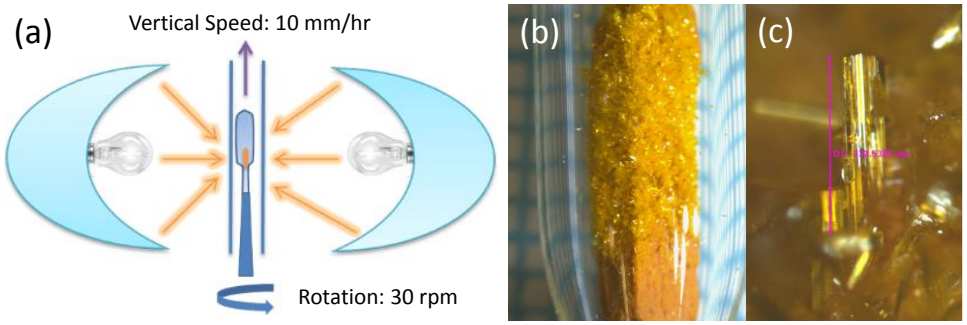

Fig. 2 (a) Schematic diagram of optical floating zone for CdS crystals growth; (b), (c) the morphology of the CdS crystals.

Steady-state Photoluminescence Spectra of CdS Bulk Crystal

The photoluminescence spectra of CdS rod and CdS crystal have been collected. The laser beam (solid-state laser, 473 nm and Nd:YAG solid-state laser, 532 nm) was collimated and focused thorough a 50× or 100× objective onto the sample surface. A confocal triple-grating spectrometer (Horiba-JY T64000) was used to collect the spectra.

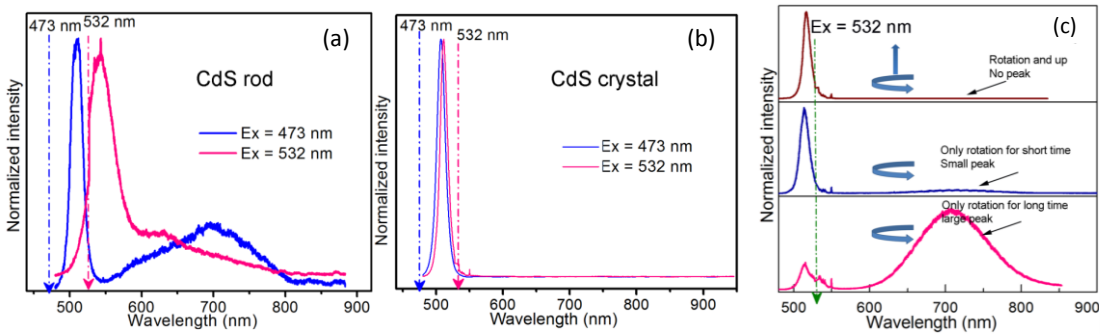

Fig. 3 The PL of the starting materials (a) and the final crystal after optical heating (b) excited by 473 nm and 532 nm, respectively. (c) The PL (excited by 532-nm laser) of CdS crystals in different growth conditions (up-movement of sample rods).

Two emission bands were usually observed in photoluminescence spectra bulk CdS. The PL spectra taken from the commercial rod before growth (Fig. 3a). Besides the sharp excitonic emission (~507 nm) near the band-edge, a broad trapped emission was located in the long wavelength (~700 nm). The origin of such defect bands is not completely understood, which is presumable from a combination of various trap states due to stoichiometric defects (interstitials or vacancies) or surface states. When excited by 532-nm laser, the CdS rod show the distinct characteristics of the trapped state emission. The large peak shift in the CdS rod spectra under different excitation wavelength should be due to the complex trapped level from impurities (Fig. 3a). In contrast, in the CdS crystal grown by this optical Bridgeman method, both Stokes and anti-Stokes emission spectrum showed the absence of the long-wavelength defect emission (Fig. 3b), while the anti-Stokes emission excited by 532-nm laser exhibits strong photoluminescence upconversion, a very important requirement towards laser cooling.

The up-movement effect of the CdS rod has also been studied in the optimized synthesis experiments. As Fig. 3c shown, if the CdS rod just kept rotation without any up-movement, the trapped state emission of final CdS crystals became larger with a longer heating time in a general trend. However, if the CdS rod kept rotation with the up-movement simultaneously, no trapped state emission at the long wavelength has been found, which indicates that the defect concentration inside the CdS crystal is low. The possible reason is that the up-movement prevents the CdS crystal from continuous high-intensity heating around the optical focus, in which the high temperature would induce more stoichiometric defects inside the crystal.

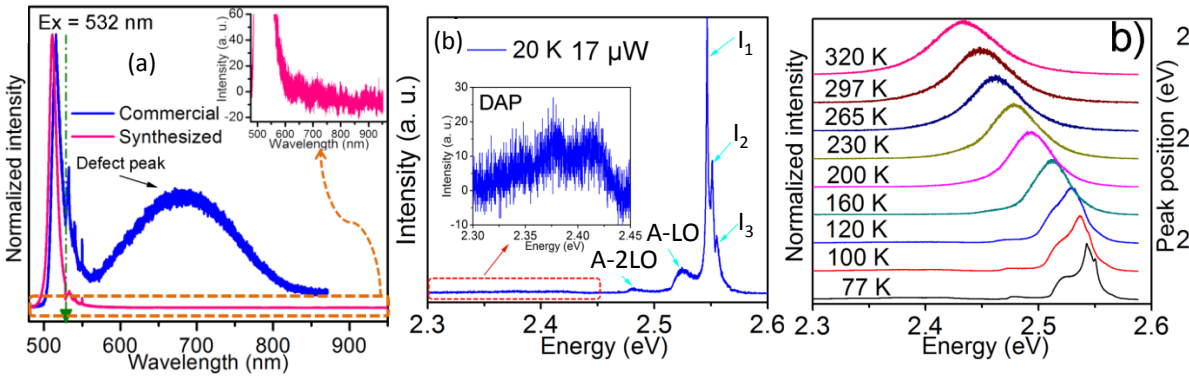

Fig. 4 (a) The comparison of PL between commecial and as-grown CdS crystals excited by 532- nm laser of 8.65 mW; (b) PL structure of CdS crystals at 20 K with a 473-nm excitation;

Compared with the spectra of commercial CdS bulk crystals (MTI Corporation), our crystals didn't show any trapped state emission. (Fig. 4a) The achievement of bulk CdS crystal without trapped state emission can be attributed to the low temperature, continuous up-movement of CdS rod and fast crystal growth rate. As Fig. 1b suggested, lower temperature for crystal growth would induce narrower non-stoichiometry. The CdS bulk crystals was grown at low lamp power (30%; 2200 ℃ at full power) on the surface of CdS rod out

of the optical focus. The temperature was low enough for good stoichiometry nature. The short time for crystal growth and continuous up-movement can prevent the overheating of CdS bulk crystals, which would induce the high defect concentration.

As we know, the donor-acceptor pair (DAP) peak, which was facilitated by sulfur vacancy and cadmium vacancy, would become noticeable compared with the bound exciton peaks under low excitation power.[23, 26-27] However, in our case the donor-acceptor pair (DAP) was very weak even with a weak excitation power around 17 μw (Fig. 4b). The weak DAP emission in the as-grown bulk CdS crystal suggests a better quality in terms of stoichiometry with less sulfur or cadmium vacancies, which may cause the large trapped state emission in long wavelength region. However, the effect of DAP emission on laser cooling of semiconductors is still not clear, as it only becomes important at lower temperatures, under which the laser cooling of semiconductors have not been studied. One possible speculation is that the DAP process could be beneficial towards pumping carriers to higher energy at low temperatures.

Results and Discussion:

In the study of laser cooling of CdS bulk crystal, the limitation on achieved net cooling is more likely to be the result of parasitic heating from unwanted impurities inside the bulk or on its surface. This problem can be avoided in CdS nanobelts, mainly due to the high crystalline quality in nanoscale, while it has remained in bulk case as the principal barrier of laser cooling for a long time. We have developed the optical floating zone to synthesize CdS bulk crystals without defect emission at long wavelength, which was attributed to the low synthesized temperature, continuous up-movement of CdS sample rod and fast crystal growth rate. In the steady-state PL spectra, the little DAP peak has confirmed the excellent stoichiometric nature and crystal quality of the as-grown CdS bulk crystal. This result largely minimize the unwanted heating induced by the long-wavelength emission during the optical process and improve the progress on the laser cooling in CdS bulk crystals. Success of controlling the defects during growth could also benefit the other applications of CdS including solar cell component, laser materials and waveguides, in which defect in the materials would impair the performance of related device, such as emission stability and work longevity.

So far, our work has discovered that the optical floating heating method can improve the solid CdS stoichiometry and crystallization quality, which has wide potential applications including purification of CdS-like materials and heat treatment of CdS-like thin film. To achieve the net laser cooling of bulk crystal, it still needs further device engineering. The achievement of net laser cooling in bulk CdS crystal may be still limited by the external quantum efficiency and the absorption efficiency, which have not been investigated for our samples. The non-radiative recombination and background absorption of materials will generate unwanted parasitic heating to prevent the achievement of net cooling, while they can not be reflected in the steady-state photoluminescence spectra. Therefore, the further step of our research may focuse on the investigation of the non-radiative process in existing as-grown crystal and improving the sample quality to reduce parasitic heating in the further systhesis, such as increasing to the external quantum efficiency and minimizing the background absorption.

Laser cooling of lead halide perovskites

(This work was supported in part by AOARD project, although it was not originally proposed in the AOARD project. We would like to include a summary into the final report)

Lead halide perovskites have garnered tremendous attention in the past few years due to their high performance as light absorbers in solar cell, and optically pumped lasers. Recent work also shows that perovskite single crystals possess low trap.-state density and high external quantum efficiency, both of which are advantageous for laser cooling if a sufficient photoluminescence upconversion could be achieved. Interestingly, indeed we find that lead halide perovskite crystals in both 3D (*i.e.,* $MAPbI_3$) and 2D (*i.e.,* $PhEPbI_4$) forms show strong photoluminescence upconversion, suggesting the possibility of laser cooling. In this work, we demonstrate experimentally that $MAPbI_3$ platelets grown by vapor phase synthesis and $PhEPbI_4$ samples exfoliated from a bulk crystal by solution synthesis can be laser cooled by ~23.0 K and 58.7 K, respectively, from room temperature.

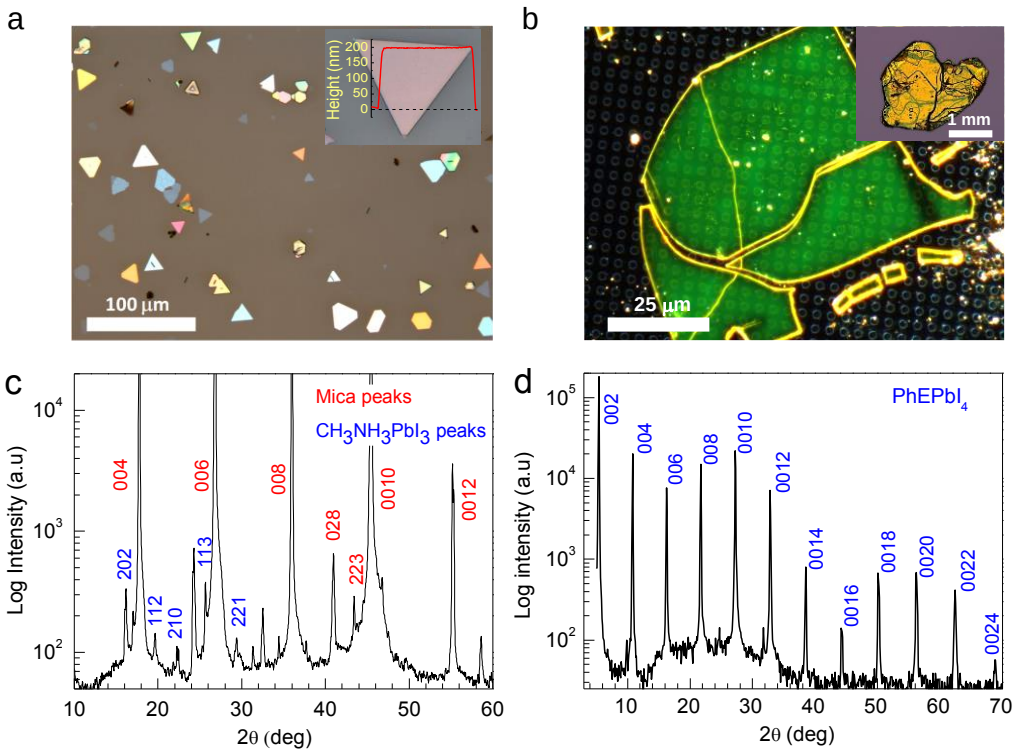

Figure 5. Morphology and Structural Characterizations of 3D and 2D perovskites. a, Optical image of as-grown $CH_3NH_3PbI_3$ 3D perovskite platelets on muscovite mica substrate. The inset displays an individual perovskite platelet with the AFM height profile. **b**, Optical image of exfoliated $PhEPbI_4$ 2D perovskite on hole-patterned silicon substrate used for laser cooling experiment. The inset: as-grown millimeter-size 2D perovskite crystal from solution. **c and d,** XRD diffraction patterns of as-grown 3D and 2D perovskites, respectively.

Figure 5a shows an optical image of $MAPbI_3$ perovskite crystals in platelet morphology on muscovite mica substrates prepared by a chemical vapor deposition (CVD) approach. The crystalline platelets exhibit tens of micrometers in size, with a thickness varied from tens of nanometers to a few micrometers. The color difference of crystals originates from their optical interference difference depending on thickness, which can be accurately determined by atomic force microscopy (AFM) and profilometry (inset to Fig. 5a). The perovskite platelet crystals synthesized by this method exhibit good crystallinity with a tetragonal phase at room temperature and a much better stability under laser illumination compared to the polycrystalline thin films which are usually obtained in solution spin-casting. Figure 5b shows an optical image of thin film of $PhEPbI_4$ exfoliated from a solution growth millimeter-sized crystal (inset to Fig. 5b). Due to the layered structure of $PhEPbI_4$, it can be readily exfoliated using Scotch tape method that provides samples with suitable thickness for the cooling experiment. Figure 5c and d are the X-ray diffraction (XRD) patterns measured for as-grown $MAPbI_3$ platelets and $PhEPbI_4$ crystals, respectively. The layered structure of 2D $PhEPbI_4$ perovskites can also be seen from XRD pattern with the periodic 002 plane peaks (Fig. 5d).
To measure the cooling effect of the crystals, we adopt the pump-probe luminescence thermometry (PPLT) technique previously used in rare-earth materials and semiconductors. The mica substrate (less than 100 μm) having perovskite crystals was suspended to isolate the sample from the copper cold finger of the cryostat. Mica exhibits excellent transparency (>95 % for 100 μm thick film at 770 nm), low refractive index (~1.6) and thermal conductivity (~0.45 W/m.K). Therefore, this design will reduce the background absorption, increase the luminescence extraction efficiency and reduce the thermal load during cooling experiment.

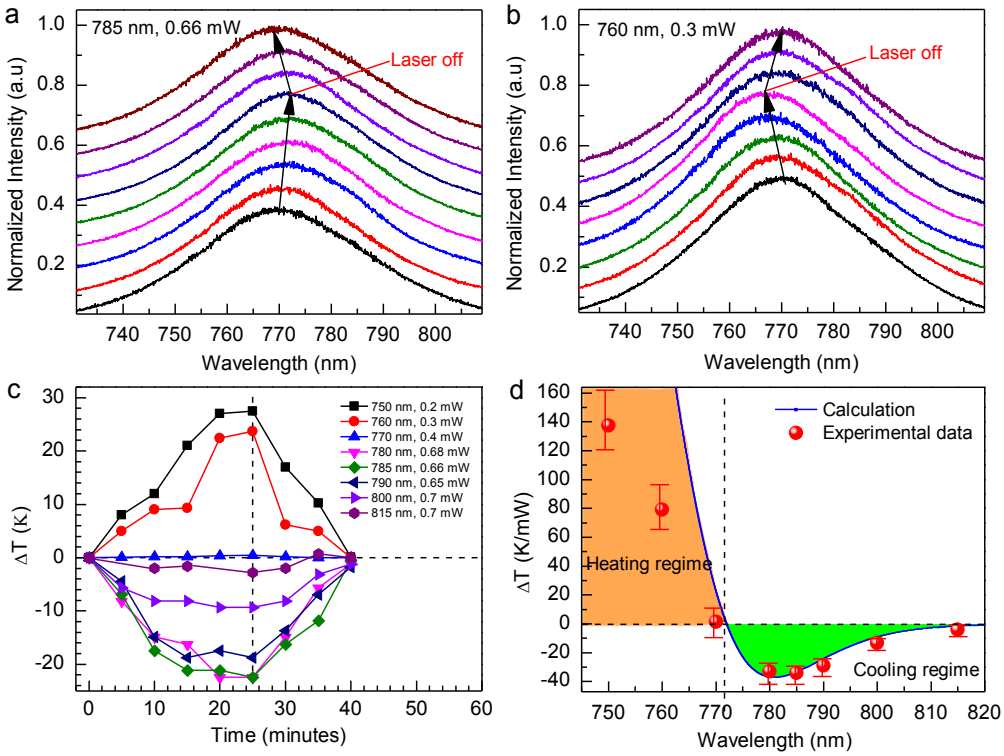

Figure 6. Net laser cooling observation in 3D perovskite $CH_3NH_3PbI_3$. a, Evolution of PPLT spectra starting from 296 K, pumped by a 785 nm laser with a power of 0.66 mW. **b**, Evolution of PPLT spectra starting from 290 K, pumped by a 760 nm laser with a power of 0.3 mW. **c**, Temperature change versus time pumped by eight laser lines (815, 800, 790, 785, 780, 770, 760, and 750 nm), using data extracted from the PPLT spectra. **d**, Summary of measured maximum ΔT (red filled-circles) and theoretically calculated temperature change (blue curve) normalized to pump power for different pump wavelengths at 296 K.

Figure 6a and Fig.6b display the evolution of photoluminescence spectra for two representative cooling and heating pumped at 785 nm and 760 nm, respectively. It is clearly seen that the photoluminescence red-shifts pumped by 785 nm, indicating a cooling process in the perovskite platelet. On the contrary, 760 nm pumping leads to blue-shifted band edge, indicating a heating process. After the pump lasers were turned off, the photoluminescence spectra returned to their original position indicating that the cooling-warming cycle is reversible. A summary of series cooling and heating experiments with different pumping wavelengths is shown in Fig.6c. The data show that the perovskite platelet crystals could be cooled by a maximum of ~23.0 K from room temperature pumped by 785 nm with a power of 0.66 mW. The normalized cooling power density (in K/mW) is plotted in Fig. 6d, showing a maximum cooling effect ~35.0 K/mW around 780-785 nm, which is much larger than that in CdS nanobelts. One possible explanation for such a big difference is the low thermal conductivity of perovskite materials. The solid curve is a theoretical calculation based on Sheik Bahae-Epstein (SB-E) theory showing a reasonable agreement, except for the heating points (at 750 and 760 nm).

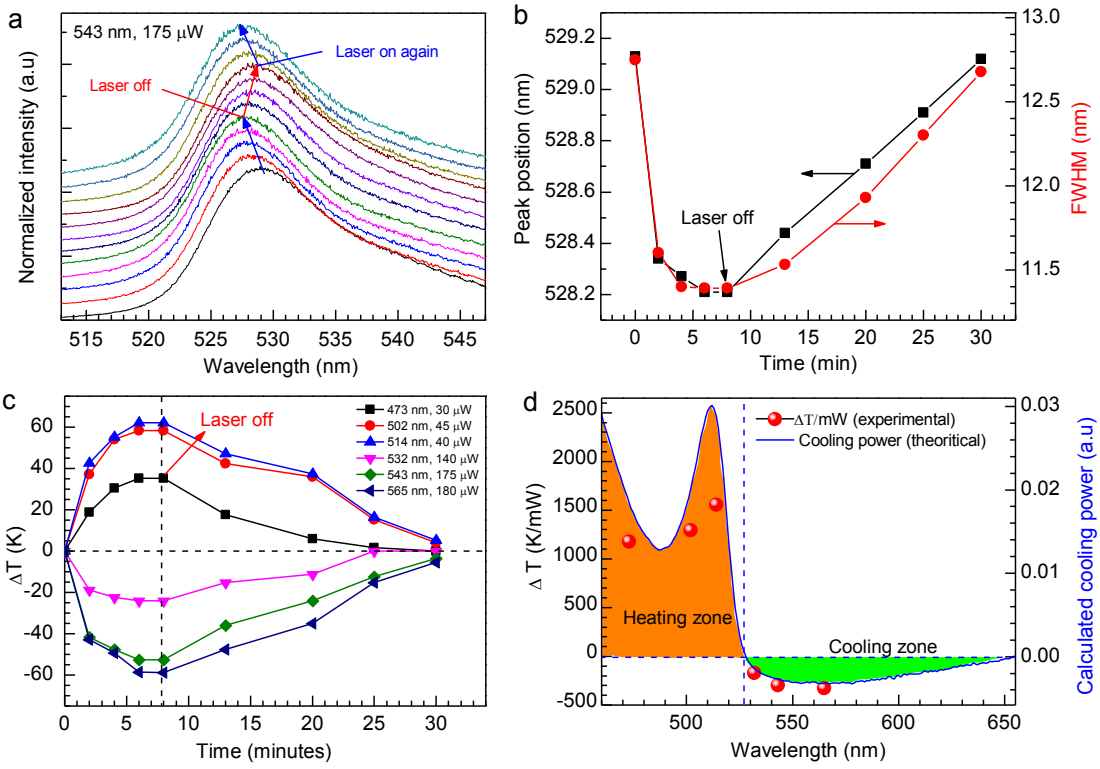

Figure 7. Net laser cooling observation in 2D perovskite ($(C_6H_5C_2H_5NH_3)_2PbI_4$). a, Evolution of PPLT spectra starting from 296 K, pumped by a 543 nm laser. The pump laser was turned on again to show that the cooling and warming process were fully reversible. **b**, The peak position and FWHM extracted from PPLT spectra during laser cooling and warming processes. **c**, Temperature change versus time pumped by six lasers (473, 502, 514, 532, 543, and 565 nm), using data extracted from the PPLT spectra. **d**, Summary of measured maximum ΔT (red-filled-circles) and theoretically calculated temperature change (blue curve) normalized to pump power for different pump wavelengths at 296 K.

Similar cooling experiment was carried out for 2D perovskite and the results are summarized in Figure 7. Fig. 7a shows the PPLT spectra of cooling-warming-cooling cycle starting from 296 K pumped by 543 nm laser. As we can see, whenever the pumping laser was on, the PPLT spectrum was blue-shifted indicating cooling of the crystal. This experiment shows that the cooling and warming process is reversible and reproducible as well. Figure 7b shows the evolution of photoluminescence peak and full width at half maximum (FWHM) of the spectra extracted from Fig. 7a for the first cooling-warming cycle. It is noted that both photoluminescence peak position and FWHM evolutions are in good agreement with the calibration curve for the 2D perovskite. This is strong evidence that the sample is indeed cooled down by the pump laser. Figure 7c and d summarize the cooling and heating of 2D perovskite crystal by various wavelength laser pumping. The maximum cooling of 58.7 K directly from room temperature was achieved with 565 nm laser excitation. The cooling and heating results also agree well with the calculation based on SB-E theory as shown in Fig. 7d.

We have demonstrated laser cooling of both 2D and 3D lead halide perovskite materials. The maximum cooling of 23.0 K and 58.7 K has been achieved for the $MAPbI_3$ and $PhEPbI_4$ perovskites, respectively. Our work expands the toolbox for optical refrigeration extensively, considering the numerous combinations of inorganic-organic perovskites. With the facile solution processing and accessible crystallization temperature of those perovskite materials, our work opens up the possibility of laser cooling devices facilely bonded to electronic and optoelectronic thermal load. The remaining challenges are to scale up the current vapor phase or solution synthesis towards a uniform macroscale crystalline film and the proper design of the heat sink, since the thermal conductivity of those perovskites is usually low.

List of Publications and Significant Collaborations that resulted from your AOARD supported project: In standard format showing authors, title, journal, issue, pages, and date, for each category list the following:

a) papers published in peer-reviewed journals,

1. D.H. Li, J. Zhang, X.J. Wang, B.L. Huang and Q.H. Xiong*, "Solid-State Semiconductor Optical Cryocooler Based on CdS Nanobelts", Nano Lett. 14(8), 4724–4728 (2014)

2. D.H. Li, Y. Liu, M. de la Mata, C. Magen, J. Arbiol, Y.P. Feng and Q.H. Xiong*, "Strain-induced spatially indirect exciton recombination in zinc-blende/wurtzite CdS heterostructures", Nano Research 8(9), 3035-3044 (2015)

3. K.Z. Du, A. Chaturvedi, X.Z. Wang, Y. Zhao, K.K. Zhang, M.I.B. Utama, P. Hu, H. Jiang, Q.H. Xiong and C. Kloc*, "Plasma-enhanced microwave solid-state synthesis of cadmium sulfide: reaction mechanism and optical properties", Dalton Trans. 44, 13444-13449 (2015)

4. S.T. Ha, C. Shen, J. Zhang and Q.H. Xiong*, "Laser cooling of organic-inorganic lead halide perovskites", Nature Photonics 10, 115–121 (2016)

5. K.Z. Du, X.Z. Wang, Y. Liu, P. Hu, M.I.B. Utama, C.K. Gan, Q.H. Xiong*, and C. Kloc*, "Weak Van der Waals Stacking, Wide-Range Band Gap, and Raman Study on Ultrathin Layers of Metal Phosphorus Trichalcogenides", ACS Nano 10(2), 1738-1743 (2016)

6. Q. Zhang, X.F. Liu, M.I.B. Utama G.C. Xing, T.C. Sum* and Q.H. Xiong*, "Phonon-Assisted Anti-Stokes Lasing in ZnTe Nanoribbons", Adv. Mater. 28, 276–283 (2016)

b) papers published in peer-reviewed conference proceedings,

Ke-zhao Du, Xingzhi Wang, Jun Zhang, Xinfeng Liu, Christian Kloc, and Qihua Xiong, "CdS Bulk Crystal Growth by Optical Floating Zone Method: Strong Photoluminescence Upconversion and Minimum Trapped State Emission", Optical Engineering, submitted, 2016 (proceeding for SPIE Photonics West "Laser cooling and Optical Refrigeration" symposium).

c) papers published in non-peer-reviewed journals and conference proceedings,

Nil

d) conference presentations without papers,

Conference name: 7th IEEE Nanoelectronics Conference (INEC 2016)
Period: 09 May 2016 to 11 May 2016
Country: China
Link: http://www.inec2016.com/
Mode: Invited Speaker

Conference name: Croucher Advanced Study Institute on 2D materials
Period: 02 May 2016 to 07 May 2016
Country: Hongkong
Link: http://www.physics.hku.hk/~croucherasi/
Mode: Session Chair

Conference name: SPIE 2016 Photonics West Conference
Period: 14 Feb 2016 to 18 Feb 2016
Country: USA
Link: http://spie.org/conferences-and-exhibitions
Mode: Attend and Chair Sessions

Conference name: MRS fall exhibit
Period: 01 Dec 2013 to 04 Dec 2013

Country: USA
Link: http://www.mrs.org/fall2013/
Mode: Attend

e) manuscripts submitted but not yet published, and

f) provide a list any interactions with industry or with Air Force Research Laboratory scientists or significant collaborations that resulted from this work.

Visited Air Force Research Laboratory at Kirtland, New Mexico, gave a presentation on laser cooling of semiconductors and discussed possible collaborations with researchers at the laboratory.

Attachments: Publications a), b) and c) listed above if possible.